# Tree Species Identification *via* $^{1}$H NMR Fingerprinting of Supercritical Carbon Dioxide Wood Extractives

Laura G. Raymond,[a,*] David Sandquist,[b] Stefan J. Hill,[a] Roger Meder,[c,d] and Volker C. Behr [e]

Six tree species were examined using $^{1}$H NMR spectroscopy of sap extracted by supercritical $CO_2$. A metabolomic approach was developed to evaluate the sap extracted from sapwood of Norway spruce (*Picea abies*), Sitka spruce (*Picea sitchensis*), radiata pine (*Pinus radiata*), macrocarpa (*Cupressus macrocarpa*), and two Eucalyptus species—shining gum and mountain ash (*Eucalyptus nitens* and *Eucalyptus regnans*. The sap extraction patterns in the different species were visualised using $^{1}$H magnetic resonance imaging. In softwoods with distinct annual rings, water was first removed from the latewood bands, and then gradually from the earlywood bands. In the case of the hardwood species an almost random water redistribution, rather than water expulsion, was observed. Analysis of the principal component analysis loading plots showed that the significant differences in the sap between each species were due to the carbohydrate region. Key discriminators were identified as pinitol, sucrose, glucose, and fructose.

*Keywords: Wood metabolites; NMR fingerprinting; Magnetic resonance imaging; Wood anatomy; Supercritical carbon dioxide*

*Contact information: a: Scion, Te Papa Tipu Innovation Park, 49 Sala St, Rotorua 3046, New Zealand; b: VTT Technical Research Centre of Finland Ltd, P.O. Box 1000, 02044 VTT, Finland; c: Meder Consulting, PO Box 3185, Bracken Ridge, QLD 4017, Australia; d: Forest Industries Research Centre, University of the Sunshine Coast, Sippy Downs, QLD 4558, Australia; e: Experimental Physics 5, University of Würzburg, Am Hubland, 97074 Würzburg, Germany;*
** Corresponding author: laura.raymond@scionresearch.com*

## INTRODUCTION

Nuclear magnetic resonance (NMR) based metabolomics research has rapidly increased over the past decade into many diverse fields (Nicholson *et al*. 1999; Markley *et al*. 2017; Pontes *et al*. 2017). It is a robust, high throughput technique that needs little or no sample separation or derivatisation and is a recognised tool in a wide range of metabolomics related applications (Ward *et al*. 2010), compared with classical approaches such as microscopic identification. There has been significant research drive for NMR metabolic profiling and fingerprinting of biofluids in the medical field, and the application of metabolomics has been used to characterise biomarkers widely in disease diagnosis (Emwas *et al*. 2013), with examples such as diabetes (Maher *et al*. 2009) and inborn errors (Bamforth *et al*. 1999). These platforms aid in decision making within surgical and clinical fields (Nicholson *et al*. 1999, 2012).

Metabolomic approaches have expanded to food science to establish food quality, safety and nutrition, and in regulation of commodities such as wine (Hong 2011), juice (Spraul *et al*. 2009), and coffee (Consonni *et al*. 2012). Numerous studies have been dedicated to the assessment of the metabolomic response of plants to insects (Widarto *et*

*al*. 2006), viruses (Choi *et al*. 2006), environmental effects (Bernillon *et al*. 2013), and at developmental stages (Ali *et al*. 2011). Classification of different species and cultivars using metabolic fingerprinting within the Edelweiss genus (*Leontopodium* spp.) has been successful, where other morphological and molecular methods have been problematic (Safer *et al*. 2011).

Comparatively little investigation has been undertaken in the study of metabolites in the sapwood of trees. Recently, the metabolic differences of bark and sapwood in four Sitka spruce clones after being challenged with a fungal pathogen were investigated using $^{1}$H NMR fingerprinting. Inoculated sapwood showed lower amounts of all metabolites, while bark had increased signals in the aromatic region (Deflorio *et al*. 2012). However, comparisons between the composition and behaviour of sapwood in different species using magnetic resonance has not yet been considered.

This study demonstrates the identification of tree species based on a metabolomic fingerprinting technique, for wood sap extraction under supercritical conditions based on $^{1}$H NMR spectroscopy and multivariate statistical analysis. Sap extraction of six tree species (three softwoods and three hardwoods) was performed using Scion's oscillating supercritical carbon dioxide ($scCO_2$) extraction technology for dewatering wood (Franich *et al*. 2014). The $scCO_2$ extraction approach is ideal to obtain bioactive compounds, as the extract is conserved from contact with air and light, and uses moderate temperature (Khaw *et al*. 2017). Both wood sap flow and wood impregnation using either fluids or supercritical fluids are well known to be affected by wood anatomy (Schneider *et al*. 2006; Siau 1984). Previous studies of the wood-water relationship using supercritical carbon dioxide have investigated the movement and nature of water during the dewatering process of *Pinus radiata* using $^{1}$H and/or $^{13}$C MR imaging (Behr *et al.* 2014; Meder *et al*. 2015; Newman *et al*. 2016; Franich *et al*. 2019). The same approach was used in this study to visualise the sap flow under $scCO_2$ conditions for the six different wood anatomies investigated in this study, using a high-pressure autoclave with a $^{1}$H/$^{13}$C double-tuned resonator (Behr *et al*. 2013) to acquire $^{1}$H magnetic resonance (MR) images of the water during the extremes of the pressure cycles.

## EXPERIMENTAL

### Materials

*Wood samples for sap and extracts collection*

Wood core samples, 10 mm in diameter, were sourced in March (Autumn) from around the Rotorua region, New Zealand (38.1 °S, 176.3 °E). The species analysed are listed in Table 1. The cored samples were wrapped in plastic and stored at -20 °C for no more than two days before $scCO_2$ extraction.

**Table 1.** Wood Species Analysed

| Common Name | Latin Name | Wood Type |
|---|---|---|
| Radiata pine | *Pinus radiata* D. Don | Softwood |
| Macrocarpa | *Cupressus macrocarpa* | Softwood |
| Norway spruce | *Picea abies* | Softwood |
| Sitka spruce | *Picea sitchensis* | Softwood |
| Shining gum | *Eucalyptus nitens* | Hardwood |
| Mountain ash | *Eucalyptus regnans* | Hardwood |

*Wood samples for MR imaging*

Green sapwood samples of all the species listed in Table 1, except Norway spruce, were sourced using the green-chain of a local sawmill. Samples were cut to 15 mm (radial) × 15 mm (tangential) × 95 mm (longitudinal) and edge-chamfered to achieve a tight fit in the 20 mm internal diameter of the high-pressure MR cell (Behr *et al*. 2013). The samples were packed with a wet tissue, sealed first in plastic, then in aluminium foil, and express delivered from New Zealand to Würzburg, Germany in under five days. The green Norway spruce samples were sourced in July (summer) from the region around Trento, Italy, and cut to the same dimensions as noted above.

## Methods

*Supercritical carbon dioxide sap extraction*

The 10 mm cored green wood specimens were extracted sequentially in a 500 mL high-pressure stainless-steel cylinder fitted with an inlet port for delivering liquid $CO_2$ for establishing the supercritical phase ($T_{crit}$ =31.1 °C, $P_{crit}$ = 7.38 MPa), an outlet port for allowing exit of $CO_2$ gas, and a separate lower port for recovery of wood sap.

Supercritical $CO_2$ phase was generated using liquid $CO_2$ (99.7% pure), which was first chilled at ice-bath temperature to ensure maintenance of the liquid phase entering the pump, and then delivered through a heated water bath maintained at 50 °C to establish the supercritical phase at the target pressure of 20 MPa. A period at the target pressure, the 'hold-time' of the order of 10 minutes, was used to establish an equilibrium while the wood specimen was held in contact with $scCO_2$ at a constant pressure of 20 MPa and 50 °C. The pressure was then decreased to around 4 MPa by pumping into the storage cylinder. The lower valve was then opened to allow wood sap to flow out to be collected in a receiver.

The process was repeated as alternating pressure cycles until the sap flow diminished or ceased. At the end of each experiment, the $CO_2$ pressure was lowered to atmospheric. The wood specimens were then removed from the cylinder and the resultant aqueous sap samples were stored in 15 mL Falcon tubes at -80 °C until analysis.

*Sample preparation for NMR analysis*

The sample preparation and NMR experimental protocol were developed by optimisation of several considerations, including water suppression parameters, pH, buffer concentration, and ratio of buffer to sample. Sodium azide was added to suppress microorganism activity, and the sodium salt of 3-(trimethylsilyl)-propionate acid-$d_4$, (TSP) was used as an internal NMR standard (0 ppm).

Frozen sap samples were thawed at room temperature and mixed on a vortex mixer for one minute, after which 500 µL was transferred to a 2 mL microtube. A 500 µL aliquot of a pH 7.00 phosphate buffer mixture was added to the aqueous sap samples. This gave a final concentration of the phosphate buffer mixture of 0.1 mol $L^{-1}$, which also contained $D_2O$ (10% v/v), TSP (0.05% w/v), and sodium azide (0.05% w/v). The mixture was homogenised by vortex mixing at room temperature for one minute before an aliquot of 600 µL was transferred into a 5 mm NMR tube for analysis.

*$^1$H NMR analysis*

One-dimensional $^1$H NMR spectra of the sap samples were acquired on a Bruker Avance III 400 MHz NMR spectrometer (Bruker, Rheinstetten, Germany) using the noesygppr1d pulse sequence in the Bruker pulse sequence library, with a pre-saturation power field of 33 Hz and transmitter frequency offset (O1) at 1886.70 Hz.

The internal probe temperature was set to 300 K. The spectral data were obtained with 65k data points, a relaxation delay of 8 s and 256 scans.

After Fourier transformation, NMR data were automatically phased, baseline corrected and referenced to the TSP resonance at 0.00 ppm. The region from 4.57 to 5.20 ppm was excluded from analysis to remove variations in the suppression of the water resonance, as was the residual acetone (from earlier cleaning cycles) signal in the region from 2.20 to 2.30 ppm.

Functional group analysis was carried out by the integration of the following broad proton chemical shift ranges; 0 to 3 ppm alkyl, 3 to 5.6 ppm carbohydrate / *O*-alkyl, and 5.6 to 8.5 ppm aromatic regions. Solvent peaks were excluded where required.

Multivariate statistical analysis was performed by bucketing spectra across the region including 0.00 to 10.00 ppm using AMIX software (Bruker, Karlsruhe, Germany) with a bucket size of 0.04 ppm. Bucketed data were evaluated using principal component analysis (PCA) with a Pareto scaling method using SIMCA 14.1 software (Sartorius Stedim Data Analytics AB, Göttingen, Germany).

*$^{1}$H MR imaging*

The $^{1}$H MR imaging was performed on a Bruker Biospec 70/30 magnetic resonance imaging system operating at 7.05 T (300 MHz $^{1}$H) with an Avance AV console, using ParaVision v4 software for acquisition (Bruker, Ettlingen, Germany). The supercritical extraction was performed using a purpose-built high-pressure polyetheretherketone (PEEK) cell and birdcage radiofrequency coil (Behr *et al*. 2013).

$^{1}$H MR images were acquired using a FLASH (Fast Low Angle SHot) sequence (Haase *et al*. 1986) with a gradient echo time ($T_E$) of 3.1 ms, a repetition time ($T_R$) of 100 ms, and flip angle of $\alpha \approx 20°$ optimised for $T_1$(H) of a typical specimen (Ernst and Anderson 1966). Images used in the present paper were taken from the fifth of eight centrally located slices, or from the third slice of four, with slice thickness = 1 mm and interslice distance = 3 mm. The field of view dimensions was 20 mm × 20 mm, with a matrix size of 128×128, resulting in a voxel size of 1 mm × 156 μm × 156 μm presented as a pixel of size 156 μm × 156 μm.

A total of 16 signals were averaged for each phase encoding step, requiring 3 min of data acquisition. Profiles across rows of pixels or up columns of pixels were processed in Prospa (Version 3.12, Magritek, Wellington, New Zealand). Because FLASH uses gradient echoes rather than spin echoes, the signal strength is proportional to the concentration of water molecules with $T_2$*(H) > $T_E$ (Haase *et al*. 1986).

*Image analysis*

Greyscale images from the MR FLASH experiments were processed using Prospa. The generated images were collected, and stack-aligned in ImageJ using the SIFT algorithm (Lowe 2004), and then cropped to the sample outline.

Drying maps were calculated by comparing individual pixel values at a cut-off 80% drop in intensity from the reference image and recording the cycle at which this took place. A false colour image map was generated showing at which cycle the limit was reached.

## RESULTS AND DISCUSSION

### Difference in Sap Composition Shown by NMR Profiles

A representative spectrum shown in Fig. 1 displays a $^{1}$H NMR metabolite profile of *P. radiata*. The carbohydrate region (C2-6, 3.2 to 4.0 ppm) is highly overlapped in sap samples, as carbohydrates show complex spectra due to functional group similarity, combined with many different individual carbohydrates being present. However, the anomeric proton on C1 of many carbohydrates can be found between 4.0 and 5.6 ppm, with these signals usually being separable from the other resonances and can be used for identification and quantification (Bubb 2003).

Likewise, due to the number of extracted components, the aromatic/phenolic region (6.0 to 8.5 ppm) and alkyl region (0.0 to 3.0 ppm) also have significant peak overlap, making individual compound identification difficult (Fig. 1).

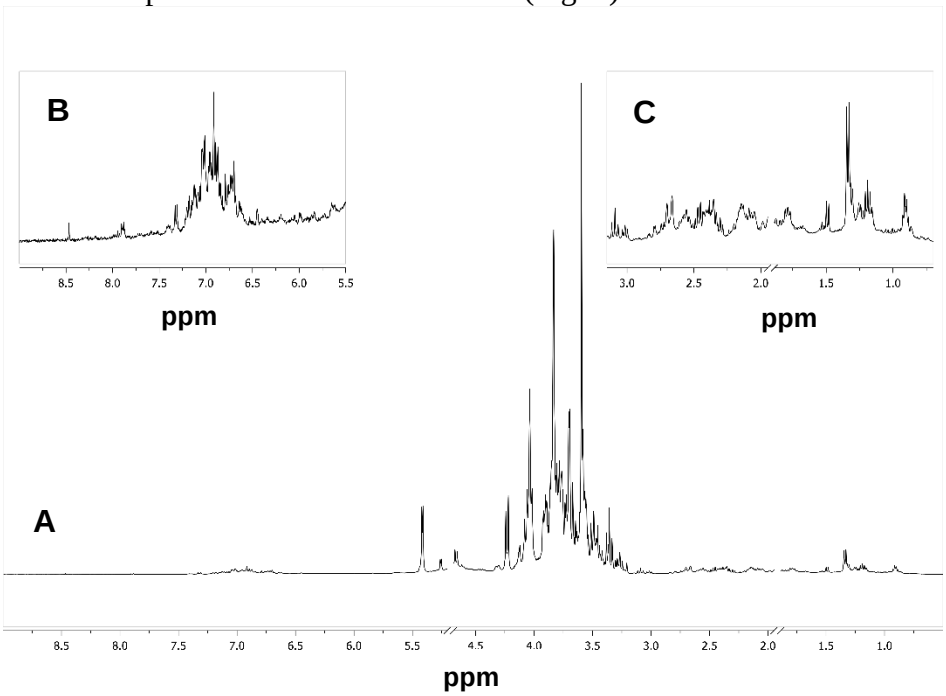


**Fig. 1.** Example $^{1}$H NMR spectra of radiata pine $scCO_2$ extracted sap showing the full spectral range dominated by carbohydrate signals (A), aromatic/phenolic region (B), and the alkyl region (C)

**Table 2.** Percentage Composition of Aromatic, Carbohydrate, and Alkyl Regions

| Species | **Aromatic** [5.6 – 8.5 ppm] | **Carbohydrate / *O*-alkyl** [3.0 – 5.6 ppm] | **Alkyl** [0.0 – 3.0 ppm] |
|---|---|---|---|
| *P. radiata* | 6.6 ± 0.1 | 83.9 ± 0.9 | 9.5 ± 0.8 |
| *C. macrocarpa* | 11.9 ± 0.2 | 70.4 ± 0.4 | 17.7 ± 0.4 |
| *P. abies* | 12.9 ± 3.2 | 71.6 ± 7.6 | 15.2 ± 6.2 |
| *P. sitchensis* | 9.6 ± 0.1 | 77.1 ± 0.2 | 13.3 ± 0.2 |
| *E. nitens* | 18.1 ± 0.6 | 66.0 ± 0.5 | 15.9 ± 1.1 |
| *E. regnans* | 16.5 ± 0.7 | 69.7 ± 0.3 | 13.8 ± 0.8 |

Note: "±" indicates the 95% confidence interval. Residual solvent peaks have been subtracted.

The proportions of aromatic, carbohydrate, and alkyl $^1$H NMR signals in the six-species investigated are presented in Table 2, showing the extent of variation in the carbohydrate content and aromatic content in particular.

## Principal Component Analysis of NMR Data

Principal component analysis (PCA) was performed on the bucketed $^1$H NMR data to obtain the maximum variation between the samples and thereby reduce the data dimensionality. This PCA model used six principal components to explain 99.7% of the variance ($R^2$ 0.997, $Q^2$ 0.99). A specialised in-house database was developed using AMIX software to give targeted screening under sample preparation conditions. This database was later applied to explore patterns and compare the experimental chemical shifts to those found by the PCA analysis. Clustering is evident in the score plot of the PCA results as displayed in Fig. 2, which highlights differences in the metabolic profile of each tree species studied.

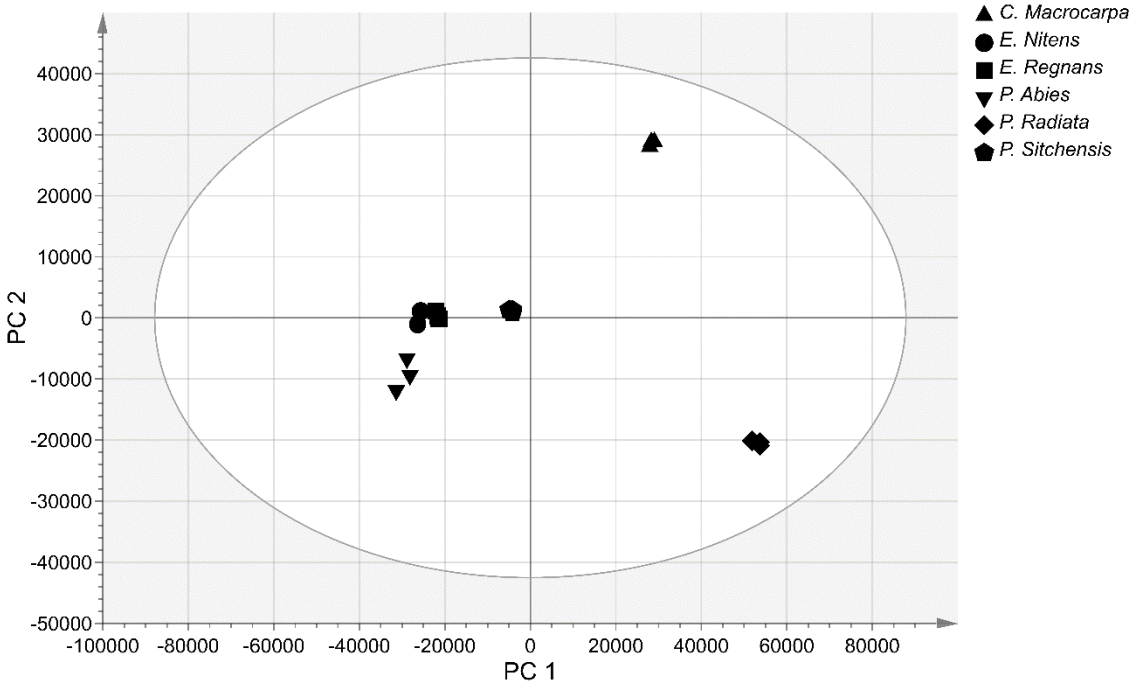


**Fig. 2.** Score plot of PCA (PC 1 vs. PC 2) results obtained from $^1$H-NMR spectra of $scCO_2$ sap extracts of the six trees involved in this study. The Hotelling T2 ellipse is shown with 95% confidence interval.

The main principal component (PC) to differentiate the species was PC 1, which explained 70.3% of the total variation. Analysis of loadings plots (not shown) found that the most influential contributions were from the carbohydrate region. Specifically, the most influential resonances were those associated with the anomeric protons of sucrose at 5.41 ppm (d, $J$ = 3.2 Hz) and fructose at 4.16 ppm (d, $J$ = 8.6 Hz).

*P. radiata* and *C. macrocarpa* were further separated by PC 2 (16.5%), with the loading plot of PC 2 (not shown) showing key variance in resonances attributed to pinitol at 4.04 ppm (t, $J$=8.5 Hz) as determined from a reference standard. *P. radiata* showed higher amounts of pinitol than the other five species. Other contributions to the differences between the species were resonances associated with the anomeric protons of α-glucose at 5.25 ppm (d, $J$ = 3.2 Hz) and β-glucose at 4.57 ppm (d, $J$= 7.9 Hz).

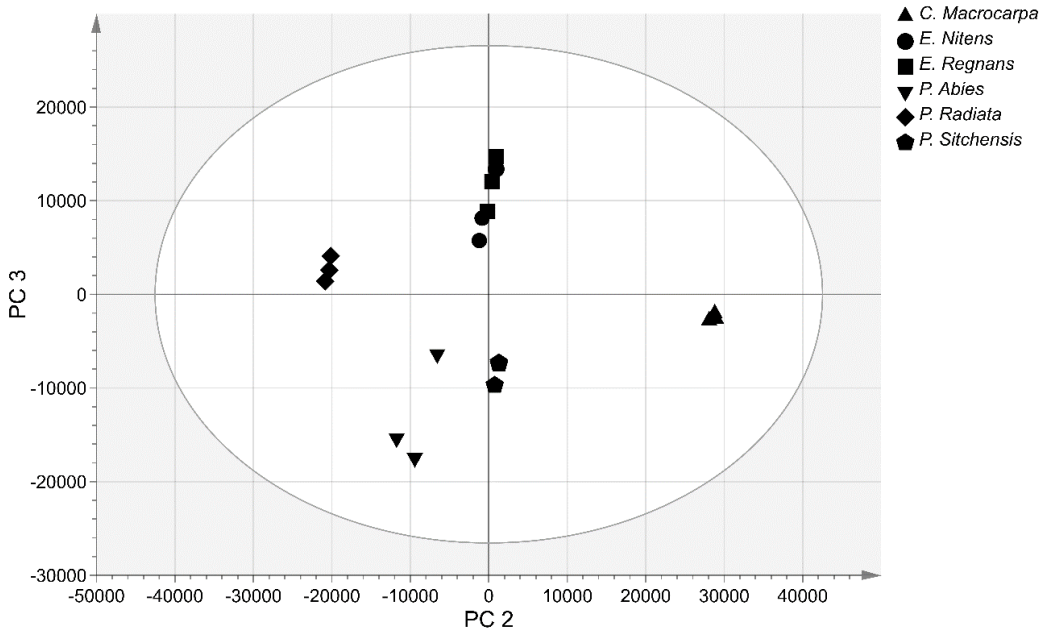


**Fig. 3.** Score plot of PCA (PC 2 vs. PC 3) results obtained from $^{1}$H-NMR spectra of $scCO_2$ sap extracts of the six trees involved in this study. The Hotelling T2 ellipse is shown with 95% confidence interval.

The PCA score plot of PC 2 *vs.* PC 3 (Fig. 3) demonstrates further separation according to similar species type along PC 3 component. The key variance for PC 3 (6.4%) were found to be due to the spectral buckets of the aromatic region. The most influential contribution was from the 7.04 to 7.08 ppm bucketed region, which was higher in both of the Eucalyptus samples.

## Correlation between MR Image Intensity and Wood Moisture Content

An empirical correlation between MR image intensity and wood moisture content was found by plotting known moisture contents against global mean image intensity (Fig. 4). A logarithmic relationship was found to describe the correlation most closely, with a $R^2$ value of 0.96, as shown in Eq. 1,

$$y=100.3*ln(x)+90.5 \quad (1)$$

The predicted cut-off moisture content was 40.5% using the FLASH routine in the present investigation. This was higher than the expected average fibre saturation point (FSP) for wood, which is approximately 30% moisture content (Babiak and Kúdela 1995; Telkki *et al*. 2013; Franich *et al*. 2019). However, as the moisture content approaches the fibre saturation point, the water in the lumens has increasingly restricted mobility. The FLASH experiments' ability to detect water signals is determined by the echo time ($T_E$). The estimated higher moisture content of 40.5% determined from Eq. 1 is therefore likely due to a shortening of the $T_2$*(H) relaxation of the water, which is attributable to increased cell wall interactions as the moisture content approaches the fibre saturation point, *i.e*., bound in cell wall micro/nano-pores (Fleury and Romero-Sarmiento 2016; Donaldson *et al*. 2018). This results in MRI signals at moisture contents lower than the true fibre saturation point being undetectable on the chosen MR imaging timescale.

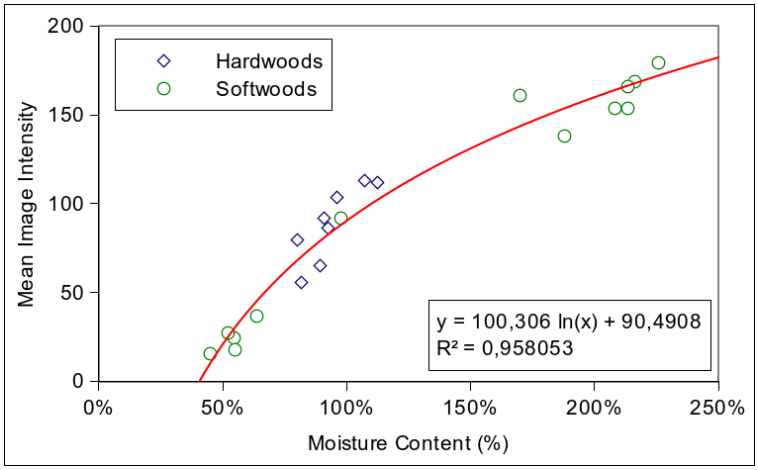


**Fig. 4.** Correlation between MR image intensity and wood moisture content. Using a logarithmic regression, the empirical cut off for MR intensity in these experiments is at a 40.6% moisture content.

## Comparing Sap Extraction for Softwoods and Hardwoods

Softwoods and hardwoods have significantly different anatomy, with softwoods consisting of fewer types of cells than hardwoods. In both hardwoods and softwoods, the sapwood component of the trunk is the main conduit for water from the roots to the crown, with a counter flow of sugar-rich sap from the crown to the rest of the tree in the cambium, just below the bark (Dinwoodie 2002).

In softwoods, the tracheids are the main conduit of water, with some influence of the rays (Siau 1984). In the case of mechanical or $scCO_2$ assisted dewatering, the resin canals, as well as effects such as earlywood/latewood transitions, also have a significant contribution to the water removal pattern. The transition between adjacent fibres is regulated by bordered pits.

In hardwoods, the vessels are the main conduit of water, with a more significant contribution of the rays due to their increased diameter and number. In the case of mechanical or $scCO_2$ assisted dewatering, the rest of the anatomy can also transport water to a lesser degree, including the fibre cells (Siau 1984).

In both hardwoods and softwoods, water flow between the different cell types is regulated by pits, which differ in their complexity and diameter. On a structurally higher level, the influence of the transition between earlywood and latewood also has a significant impact on water flow (Siau 1984).

These differences are examined here at two levels, firstly to determine any overall significant differences between the analysed hardwoods and softwoods as groups, and then for any individual differences of note.

Comparing soft- and hardwood groups, a significant difference was observed between the $4^{th}$ and $5^{th}$ dewatering cycle, as shown in Fig. 5. For hardwoods, there was a relative drop of relative moisture content from 100 to 60%, where it began to plateau, while for softwoods the moisture content continued to reduce to 40% before plateauing, as has been previously observed (Dawson and Pearson 2017). In softwoods, this is attributed to the sap removal *via* mechanical transportation (or redistribution) of water through the less saturated latewood bands (Fig. 6). In hardwoods, on the other hand, vessels are the main longitudinal conduit of water, with the pit structure limiting transverse transportation (Cronshaw 1960). Considering this, most of the sap loss is attributed to longitudinal removal, with only subsequent limited redistribution of water in the transverse plane.

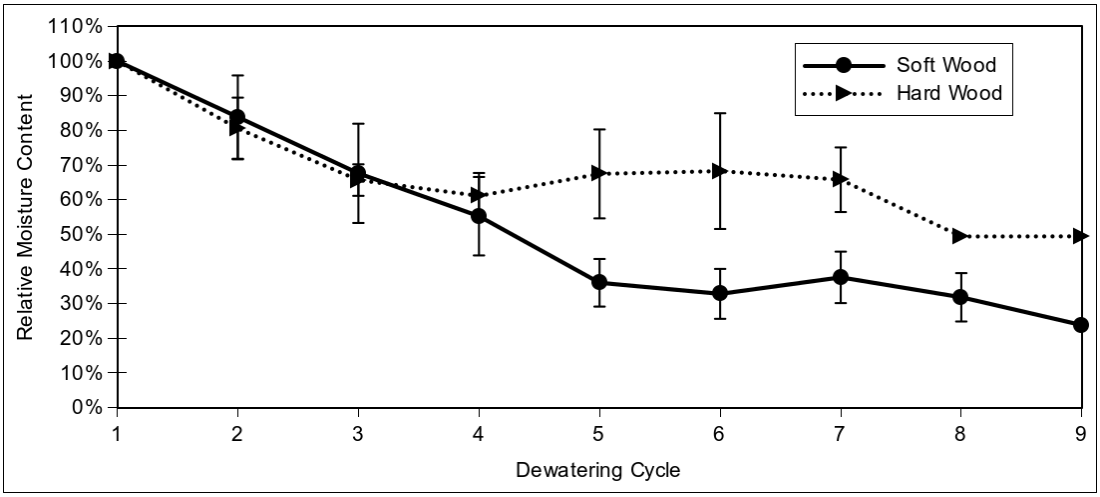


**Fig. 5.** Comparison of the average water extraction per cycle between hardwood and softwood (n = 8 soft woods, n = 4 hard woods, error bars = SD)

## Anatomical Effects on Sap Extraction

The individual dewatering MR imaging results are shown in Fig. 6. *P. radiata*, *P. abies*, and *P. sitchensis* showed evidence of clear water transport through the latewood bands. *C. macrocarpa* showed a much more disordered water loss mechanism, while *E. regnans* and *E. nitens* showed a much more limited water loss, with *E. nitens* showing water redistribution without expulsion. Softwoods with defined latewood bands, such as *P. radiata*, *P. abies* and *P. sitchensis*, were characterised by having a lower moisture content than the earlywood. For these species, a clear mechanism is apparent, with water transport from the earlywood to the latewood, which presumably is then mechanically transported out along the radial latewood faces of the samples (Meder *et al.* 2003, 2015).

By comparison, *C. macrocarpa* does not have well-defined latewood bands and presents a very different mechanism. The interpretation is that there is successively deeper penetration and dissolution of $CO_2$ into the sample until gas bubble pressure in the centre is generated at the trough of the pressure cycle to force the water out through the earlywood structure.

The two hardwoods analysed in this study, *E. regnans* and *E. nitens*, belong to the ash group of *Eucalyptus* (Dadswell 1972; Haslett 1988). Both species are known to be difficult to dry, with severe internal collapse, (checking), as well as surface checking and cupping (Haslett 1988; Dawson and Pearson 2017). An example of this checking can be seen in the light microscopy illustration for *E. nitens* in Fig. 6. For other species of the group (*E. delegatensis*), these effects are known to be aggravated if temperatures exceed 30 °C in the initial stages of drying (Dadswell 1972). The anatomical properties such as vessel size and distribution (Ilic 1991), number of tyloses, pit types and distribution (Cronshaw 1960; Dadswell 1972), of both species are very similar. The tyloses present have been categorised as "lesser amounts down to very sparse" (Dadswell 1972). However, it was consistently observed that less water was removed from *E. nitens* than *E. regnans* across all sampled trees. This difference may relate to the presence of tyloses or potentially to mechanical effects due to differences in internal structure collapse.

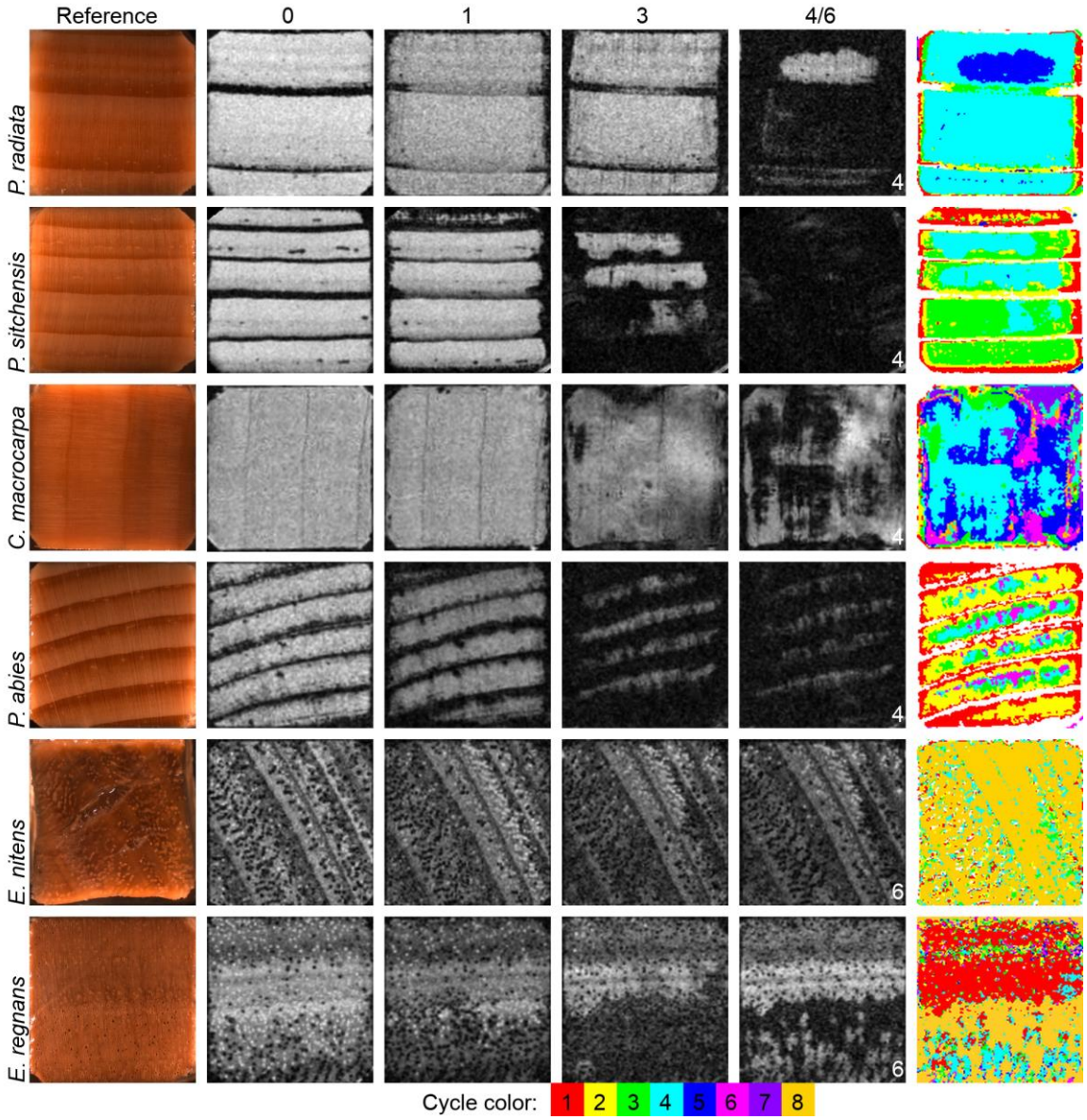


**Fig. 6.** First column; light microscopy reference. Second to fifth column; FLASH routine MRI imaging at the apex of the pressure cycle. Sixth column; colour coded overlay showing the cycle at which an individual pixel falls below 80% of its original intensity.

## Industrial Potential of Identified Metabolites

The $scCO_2$ sap extraction has been shown to give the highest selectivity towards sugars such as sucrose, pinitol, and $\alpha$- and $\beta$-glucose, based on the different wood species studied. These are all highly water-soluble metabolites, with potentially some fractionation occurring as an effect of the differences in extraction mechanism and path. Beyond the described method being used as a fingerprinting platform, utilising $scCO_2$ extraction (Demirbas 2001), these isolated metabolites can have significant industrial applications as chemical precursors. Beyond being used on their own, sucrose and glucose are used as precursors in several processes including production of glutamic acid and lactic acid (Isikgor and Becer 2015). Pinitol has potential use in several applications in medical (Narayanan *et al*. 1987) and metabolic application fields (Ostlund and Sherman 1996).

## CONCLUSIONS

1. Tree species can be identified from wood sap isolated *via* $scCO_2$ extraction with the application of metabolomics in combination with multivariate statistical analysis.
2. Sap drainage patterns differ significantly between hard- and softwoods under $scCO_2$ extraction, which may contribute to the identified differences in sap chemical composition.
3. A plethora of aliphatic and aromatic compounds were extracted under mild temperatures, that with separation and identification of individual compounds could feed into high value chemical industries or act as potential biomarkers, opening the possibility of employing them as a diagnostics tool.

## ACKNOWLEDGMENTS

This work was funded by the Ministry of Business, Innovation and Employment, through Crown Research Institute (CRI) Core Funding to Scion. The authors would like to thank the technical assistance provided by Sheree Anderson (Scion), Hank Kroese (Scion), Daniel Van De Pas (Scion), and Sabine Voll (Universität Würzburg) for help with both the experimental setup and sourcing of the wood materials. The authors acknowledge Drs. Jakub and Anna Sandak at IVALSA, Italy, for the supply of the Norway spruce sample to the Universität Würzburg. Roger Meder would like to acknowledge travel assistance from the JW Gottstein Memorial Trust and the Deutsche Akademischer Austauschdienst for travel during the period 2011 to 2013.

## REFERENCES CITED

Ali, K., Maltese, F., Fortes, A. M., Pais, M. S., Choi, Y. H., and Verpoorte, R. (2011). "Monitoring biochemical changes during grape berry development in Portuguese cultivars by NMR spectroscopy," *Food Chemistry* 124(4), 1760-1769. DOI: 10.1016/j.foodchem.2010.08.015

Babiak, M., and Kúdela, J. (1995). "A contribution to the definition of the fiber saturation point," *Wood Science and Technology* 29(3). DOI: 10.1007/bf00204589

Bamforth, F., Dorian, V., Vallance, H., and Wishart, D. (1999). "Diagnosis of inborn errors of metabolism using $^{1}H$ NMR spectroscopic analysis of urine," *Journal of Inherited Metabolic Disease* 22(3), 297-301. DOI: 10.1023/A:1005531432766

Behr, V. C., Schmid, M. W., Franich, R. A., and Meder, R. (2013). "An advanced, integrated large-volume high-pressure autoclave and $^{1}H/^{13}C$ double-tuned resonator for chemistry and materials nuclear magnetic resonance spectroscopy and microscopy investigations: NMR spectroscopy and microscopy at high pressures," *Concepts in Magnetic Resonance Part B: Magnetic Resonance Engineering* 43(2), 49-58. DOI: 10.1002/cmr.b.21233

Behr, V. C., Hill, S. J., Meder, R., Sandquist, D., Hindmarsh, J. P., Franich, R. A., and Newman, R. H. (2014). "Carbon-13 NMR chemical-shift imaging study of dewatering of green sapwood by cycling carbon dioxide between supercritical fluid and gas phases," *The Journal of Supercritical Fluids*, 95, 535-540. DOI:

10.1016/j/supflu.2014.08.026

Bernillon, S., Biais, B., Deborde, C., Maucourt, M., Cabasson, C., Gibon, Y., Hansen, T. H., Husted, S., de Vos, R. C., Mumm, R., and others. (2013). "Metabolomic and elemental profiling of melon fruit quality as affected by genotype and environment," *Metabolomics* 9(1), 57-77. DOI: 10.1007/s11306-012-0429-1

Bubb, W. A. (2003). "NMR spectroscopy in the study of carbohydrates: Characterizing the structural complexity," *Concepts in Magnetic Resonance* 19A(1), 1-19. DOI: 10.1002/cmr.a.10080

Choi, Y. H., Kim, H. K., Linthorst, H. J. M., Hollander, J. G., Lefeber, A. W. M., Erkelens, C., Nuzillard, J.-M., and Verpoorte, R. (2006). "NMR metabolomics to revisit the tobacco mosaic virus infection in *Nicotiana tabacum* leaves," *Journal of Natural Products* 69(5), 742-748. DOI: 10.1021/np050535b

Consonni, R., Cagliani, L. R., and Cogliati, C. (2012). "NMR based geographical characterization of roasted coffee," *Talanta* 88, 420-426. DOI: 10.1016/j.talanta.2011.11.010

Cronshaw, J. (1960). "The fine structure of the pits of *Eucalyptus regnans* (F. Muell.) and their relation to the movement of liquids into the wood," *Australian Journal of Botany* 8(1), 51-57. DOI: 10.1071/BT9600051

Dadswell, H. E. (1972). *The Anatomy of Eucalypt Woods* (Technological Paper), Forest Products Laboratory, Division of Applied Chemistry, Commonwealth Scientific and Industrial Research Organization, Australia, Melbourne.

Dawson, B. S. W., and Pearson, H. (2017). "Effect of supercritical $CO_2$ dewatering followed by oven-drying of softwood and hardwood timbers," *Wood Science and Technology* 51(4), 771-784. DOI: 10.1007/s00226-017-0895-8

Deflorio, G., Horgan, G., Jaspars, M., and Woodward, S. (2012). "Defense response of Sitka spruce before and after inoculation with *Heterobasidion annosum*: $^{1}$H NMR fingerprinting of bark and sapwood metabolites," *Analytical and Bioanalytical Chemistry* 402(10), 3333-3344. DOI: 10.1007/s00216-011-5666-z

Demirbas, A. (2001). "Supercritical fluid extraction and chemicals from biomass with supercritical fluids," *Energy Conversion & Management* 42(3), 279-294. DOI: 10.1016/S0196-8904(00)00059-5

Dinwoodie, J. (2002). *Timber: Its Nature and Behaviour*, CRC Press, Boca Raton, FL, USA.

Donaldson, L. A., Cairns, M., and Hill, S. J. (2018). "Comparison of micropore distribution in cell walls of softwood and hardwood xylem," *Plant Physiology* 178(3), 1142–53. DOI: 10.1104/pp.18.00883

Emwas, A.-H. M., Salek, R. M., Griffin, J. L., and Merzaban, J. (2013). "NMR-based metabolomics in human disease diagnosis: applications, limitations, and recommendations," *Metabolomics*, 9(5), 1048-1072. DOI: 10.1007/s11306-013-0524-y

Fleury, M., and Romero-Sarmiento, M. (2016). "Characterization of shales using T1-T2 NMR maps," *Journal of Petroleum Science and Engineering* 137, 55-62. DOI: 10.1016/j.petrol.2015.11.006

Franich, R. A., Gallagher, S., and Kroese, H. (2014). "Dewatering green sapwood using carbon dioxide cycled between supercritical fluid and gas phase," *The Journal of Supercritical Fluids* 89, 113-118. DOI: 10.1016/j.supflu.2014.02.019

Franich, R. A., Meder, R., Falge, M., Fuchs, J., and Behr, V. C. (2019). "Uncovering supercritical $CO_2$ wood dewatering *via* interleaved $^{1}$H-imaging and $^{13}$C-spectroscopy with real-time reconstruction," *The Journal of Supercritical Fluids* 114, 56-62. DOI:

10.1016/j.supflu.2018.10.006

Haslett, A. N. (1988). *Properties and Utilisation of Exotic Speciality Timbers Grown in New Zealand Part V: Ash Eucalypts and Eucalyptus Nitens* (FRI Bulletin no. 119), Scion, Rotorua, New Zealand.

Hong, Y.-S. (2011). "NMR-based metabolomics in wine science," *Magnetic Resonance in Chemistry* 49, S13-S21. DOI: 10.1002/mrc.2832

Ilic, J. (1991). *CSIRO Atlas of Hardwoods*, Springer-Verlag, Berlin.

Isikgor, F. H., and Becer, C. R. (2015). "Lignocellulosic biomass: A sustainable platform for the production of bio-based chemicals and polymers," *Polymer Chemistry* 6(25), 4497-4559. DOI: 10.1039/C5PY00263J

Khaw, K. Y., Parat, M. O., Shaw, P. N., and Falconer, J. R. (2017). "Solvent supercritical fluid technologies to extract bioactive compounds from natural sources: A review," *Molecules* 22(7), 1186-1208. DOI:10.3390/molecules22071186

Lowe, D. G. (2004). "Distinctive image features from scale-invariant keypoints," *International Journal of Computer Vision* 60(2), 91-110. DOI: 10.1023/b:visi.0000029664.99615.94

Maher, A. D., Lindon, J. C., and Nicholson, J. K. (2009). "$^{1}$H NMR-based metabonomics for investigating diabetes," *Future Medicinal Chemistry* 1(4), 737-747. DOI: 10.4155/fmc.09.54

Markley, J. L., Brüschweiler, R., Edison, A. S., Eghbalnia, H. R., Powers, R., Rafferty, D., and Wishart, D. S. (2017). "The future of NMR-based metabolomics," *Current Opinion in Biotechnology* 43, 34-40. DOI: 10.1016/j.copbio.2016.08.001

Meder, R., Codd, S. L., Franich, R. A., Callaghan, P. T., and Pope, J. M. (2003). "Observation of anisotropic water movement in *Pinus radiata* D. Don wood using magnetic resonance micro-imaging," *Holz als Roh- und Werkstoff* 61(4), 251-256. DOI: 10.1007/s00107-003-0400-y

Meder, R., Franich, R. A., Callaghan, P. T., and Behr, V. C. (2015). "A comparative study of dewatering of *Pinus radiata* sapwood using supercritical $CO_2$ *via in situ* magnetic resonance microimaging," *Holzforschung* 69(9), 1137-1142. DOI: 10.1515/hf-2014-0134

Narayanan, C., Joshi, D., Mujumdar, A., and Dhekne, V. (1987). "Pinitol—A new anti-diabetic compound from the leaves of *Bougainvillea spectabilis*," *Current Science* 56(3), 139-141.

Newman, R. H., Franich, R. A., Meder, R., Hill, S. J., Kroese, H., Sandquist, D., Hindmarsh, J. P., Schmid, M. W., Fuchs, J. and Behr, V. C. (2016). "Proton magnetic resonance imaging used to investigate dewatering of green sapwood by cycling carbon dioxide between supercritical fluid and gas phases," *The Journal of Supercritical Fluids* 111, 36-42. DOI: 10.1016/j/supflu.2016.01.007

Nicholson, J. K., Holmes, E., Kinross, J. M., Darzi, A. W., Takats, Z., and Lindon, J. C. (2012). "Metabolic phenotyping in clinical and surgical environments," *Nature*, 491(7424), 384-392. DOI: 10.1038/nature11708

Nicholson, J. K., Lindon, J. C., and Holmes, E. (1999). " 'Metabonomics': Understanding the metabolic responses of living systems to pathophysiological stimuli *via* multivariate statistical analysis of biological NMR spectroscopic data," *Xenobiotica*, 29(11), 1181-1189. DOI: 10.1080/004982599238047

Ostlund, R. E., and Sherman, W. R. (1996). "Pinitol and derivatives thereof for the treatment of metabolic disorders," U. S. Patent No. US5827896A.

Pontes, J. G. M., Brasil, A. J. M., Cruz, G. C. F., de Souza, R. N., and Tasic, L. (2017)

"NMR-based metabolomics strategies: Plants, animal and humans," *Analytical Methods* 9, 1078-1096. DOI: 10.1039/C6AY03102A

Safer, S., Cicek, S. S., Pieri, V., Schwaiger, S., Schneider, P., Wissemann, V., and Stuppner, H. (2011). "Metabolic fingerprinting of *Leontopodium* species (Asteraceae) by means of $^{1}$H NMR and HPLC–ESI-MS," *Phytochemistry* 72(11–12), 1379-1389. DOI: 10.1016/j.phytochem.2011.04.006

Schneider, P. F., Levien, K. L., and Morrell, J. J. (2006). "Effect of wood characteristics on pressure responses during supercritical carbon dioxide treatment," *Wood and Fiber Science* 38(4), 660-671.

Siau, J. F. (1984). *Transport Processes in Wood*, Springer-Verlag, Berlin.

Spraul, M., Schütz, B., Humpfer, E., Mörtter, M., Schäfer, H., Koswig, S., and Rinke, P. (2009). "Mixture analysis by NMR as applied to fruit juice quality control," *Magnetic Resonance in Chemistry* 47(S1), S130-S137. DOI: 10.1002/mrc.2528.

Telkki, V.-V., Yliniemi, M., and Jokisaari, J. (2013). "Moisture in softwoods: Fiber saturation point, hydroxyl site content, and the amount of micropores as determined from NMR relaxation time distributions," *Holzforschung* 67(3), 291-300. DOI: 10.1515/hf-2012-0057

Ward, J. L., Baker, J. M., Miller, S. J., Deborde, C., Maucourt, M., Biais, B., Rolin, D., Moing, A., Moco, S., Vervoort, J., Lommen, A., Schäfer, H., Humpfer, E., and Beale, M. H. (2010). "An inter-laboratory comparison demonstrates that $^{1}$H-NMR metabolite fingerprinting is a robust technique for collaborative plant metabolomic data collection," *Metabolomics* 6(2), 263-273. DOI: 10.1007/s11306-010-0200-4

Widarto, H. T., Van Der Meijden, E., Lefeber, A. W. M., Erkelens, C., Kim, H. K., Choi, Y. H., and Verpoorte, R. (2006). "Metabolomic differentiation of *Brassica rapa* following herbivory by different insect instars using two-dimensional nuclear magnetic resonance spectroscopy," *Journal of Chemical Ecology* 32(11), 2417-2428. DOI: 10.1007/s10886-006-9152-6

Article submitted: July 4, 2019; Peer review completed: December 7, 2019; Revised version received and accepted: February 2, 2020; Published: February 11, 2020.
DOI: 10.15376/biores.15.2.2371-2384